



Titania Nanotubes-Bonded Sulfamic Acid as an Efficient Heterogeneous Catalyst for the Synthesis of *n*-Butyl Levulinate

Shuolin Zhou^{1*}, Min Lei¹, Junzhuo Bai¹, Xianxiang Liu^{2*}, Lu Wu¹, Min Long¹, Keying Huang¹ and Dulin Yin²

¹School of Elementary Education, Changsha Normal University, Changsha, China, ²National and Local Joint Engineering Laboratory for New Petro-chemical Materials and Fine Utilization of Resources, Key Laboratory of the Assembly and Application of Organic Functional Molecules of Hunan Province, College of Chemistry and Chemical Engineering, Hunan Normal University, Changsha, China

OPEN ACCESS

Edited by:

Subhamay Pramanik,
University of Kansas, United States

Reviewed by:

Amit Kumar,
University of Pennsylvania,
United States
Anupam Singha Roy,
Palacky University Olomouc, Czechia

*Correspondence:

Shuolin Zhou
slzhou1989@163.com
Xianxiang Liu
lxx@hunnu.edu.cn

Specialty section:

This article was submitted to
Catalytic Reactions and Chemistry,
a section of the journal
Frontiers in Chemistry

Received: 12 March 2022

Accepted: 01 April 2022

Published: 02 May 2022

Citation:

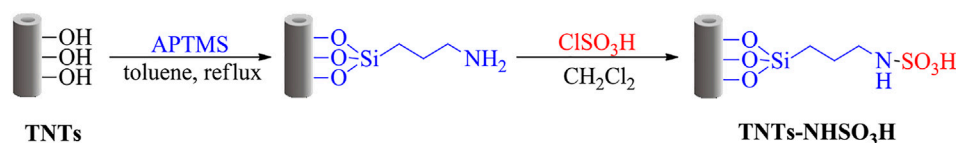
Zhou S, Lei M, Bai J, Liu X, Wu L,
Long M, Huang K and Yin D (2022)
Titania Nanotubes-Bonded Sulfamic
Acid as an Efficient Heterogeneous
Catalyst for the Synthesis of *n*-
Butyl Levulinate.
Front. Chem. 10:894965.
doi: 10.3389/fchem.2022.894965

The titania nanotubes-bonded sulfamic acid (TNTs-NHSO₃H) catalyst was designed and successfully fabricated by the post-synthesis modification method. The as-prepared catalyst was characterized by a variety of characterization techniques, including Fourier transform infrared (FT-IR) spectroscopy, X-ray photoelectron spectroscopy (XPS), transmission electron microscopy (TEM), scanning electron microscopy (SEM), X-ray diffraction (XRD) analysis, and thermogravimetry-differential thermal gravimetry (TG-DTG). The crystal structure of the TNTs still maintained during the modification process. Although the BET surface area was decreased, the amount of Brønsted acid sites can be efficiently fabricated on the TNTs. The catalytic activity of TNTs-NHSO₃H was examined for the synthesis of *n*-butyl levulinate (BL) from levulinic acid (LA) and furfuryl alcohol (FA). A relatively high selectivity (99.6%) at 99.3% LA conversion was achieved for esterification of levulinic acid owing to the strong Brønsted acidity sites. And also, the TNTs-NHSO₃H catalyst exhibited a higher reactivity for alcoholysis of FA and the yield of BL reached 90.4% with 100% FA conversion was obtained under the mild conditions.

Keywords: TiO₂ nanotubes, heterogeneous catalyst, levulinate esters, esterification, alcoholysis

INTRODUCTION

The increasing worldwide fossil fuel consumption and the increasing greenhouse gases emission and other environmental hazards have prompted people to seek other energy sources. The efficient conversion of available and diverse biomass resources into biofuel is an attractive and promising strategy (Gaurav et al., 2017; Alonso et al., 2010). Levulinate esters (LAEs), as a typical representative derived from the bio-based feedstock, have received significant attention. Because they have strong stability, high lubricity, good fluidity, and low combustion oxygen demand, which are similar to fatty acid methyl esters in biodiesel (Christensen et al., 2011). In addition, levulinate esters are one of the most potential platform compounds since their molecular structure contains a carbonyl and ester groups which have high reactivity and can be further applied to produce many important chemicals, such as γ -valerolactone (Zhang et al., 2020) and pyrrolidone (Shen et al., 2019). Furthermore, alkyl levulinates are also the crucial chemicals for other industrially important applications, such as green solvents, plasticizers, and flavoring agents (Wu et al., 2021). Hence, the synthesis of levulinate esters



SCHEME 1 | Preparation steps for fabricating titania nanotubes-bonded sulfamic acid.

has received abundant attention in recent years from academia and industry, and increasing effort has been devoted to the development of synthetic pathways, the design of novel and efficient catalysts, and optimizing the catalytic process (Démolis et al., 2014).

Up to now, there are several developed potential pathways for the synthesis of LAEs in the presence of various acid catalysts (Tian et al., 2021; Liu et al., 2020). Commercially the acid-catalyzed reactions are largely carried out by different mineral acidic catalysts such as H_2SO_4 , HCl , and H_3PO_4 , which often suffer from severe corrosion, product separation and purification, waste, and safety problems. From the practical point of view, readily separated and recovered heterogeneous catalysts, therefore, are more environmentally friendly would be desirable. Among heterogeneous catalysts, TiO_2 nanotubes (TNTs) materials have attracted extensive attention owing to their chemical stability, large surface area, non-toxicity, and low production cost (Roy et al., 2011). In the past few years, TNTs synthesized by a simple alkaline hydrothermal treatment have been used as a solid acid catalyst for various acid-catalyzed organic transformations (Kitano et al., 2010; Li et al., 2015; de Carvalho et al., 2017). The amount and strength of origin acid sites on the TNTs, however, would be limited in the catalytic applications (Adeyeye et al., 2021). It is worth noting that TNTs have a high concentration of hydroxyl groups ($-\text{OH}$) on the surface, which makes them flexible in functionalization with a wide range of organic groups, particular with organosiloxane agents. 3-Aminopropyltrimethoxysilane (APTMS) (Duong et al., 2018), 3-aminopropyltriethoxysilane (APTES) (Pontón et al., 2014), [1-(2-amino-ethyl)-3-aminopropyl]trimethoxy silane (AAPTS) (Wang et al., 2013), octadecyltrimethoxysilane (OTS) (Chao et al., 2013), and octadecyltrichlorosilane (ODS) (Niu and Cai, 2009) have been reported in the literature as chemical modifiers of the TNT surface. Furthermore, hydrothermally synthesized TNTs can be further functionalized by the integration of acidic functional groups to increase the acidity of TNTs in our previous work (Zhou L. et al., 2018; Zhou et al., 2019; Zhou et al., 2022). These studies mean that TNTs as a support material that can be rationally designed and modified as a much higher performance solid acid catalyst, which would bring a wide range of catalytic applications. Moreover, hybrid organic-inorganic materials in the catalytic reaction can provide a synergic and cooperative behavior toward chemo selective and favorable products with high yields (Wight and Davis, 2002).

In pursuit of our recent studies to develop hybrid organic-inorganic solid acid catalysts, the TiO_2 nanotubes surface was first functionalized with NH_2 groups through the APTMS grafting and the SO_3H groups were covalently linked to surface NH_2 groups by using chlorosulfonic acid as a sulfonating reagent. In

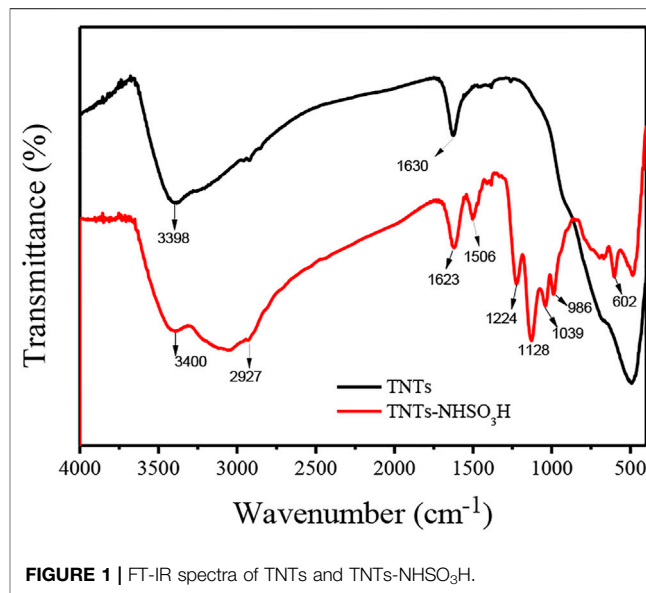


FIGURE 1 | FT-IR spectra of TNTs and TNTs-NHSO₃H.

the present work, schematic procedures for surface modification on TiO_2 nanotubes through chemical treatment are presented in **Scheme 1**. The physicochemical properties of the synthesized TNTs-NHSO₃H catalyst were characterized by FT-IR, XPS, SEM, TEM, XRD, TGA, and N_2 physisorption techniques. The potential catalytic activity of TNTs-NHSO₃H was investigated in the synthesis of high value-added *n*-butyl levulinate from esterification of levulinic acid (LA) and alcoholysis of furfuryl alcohol (FA), respectively.

EXPERIMENTAL

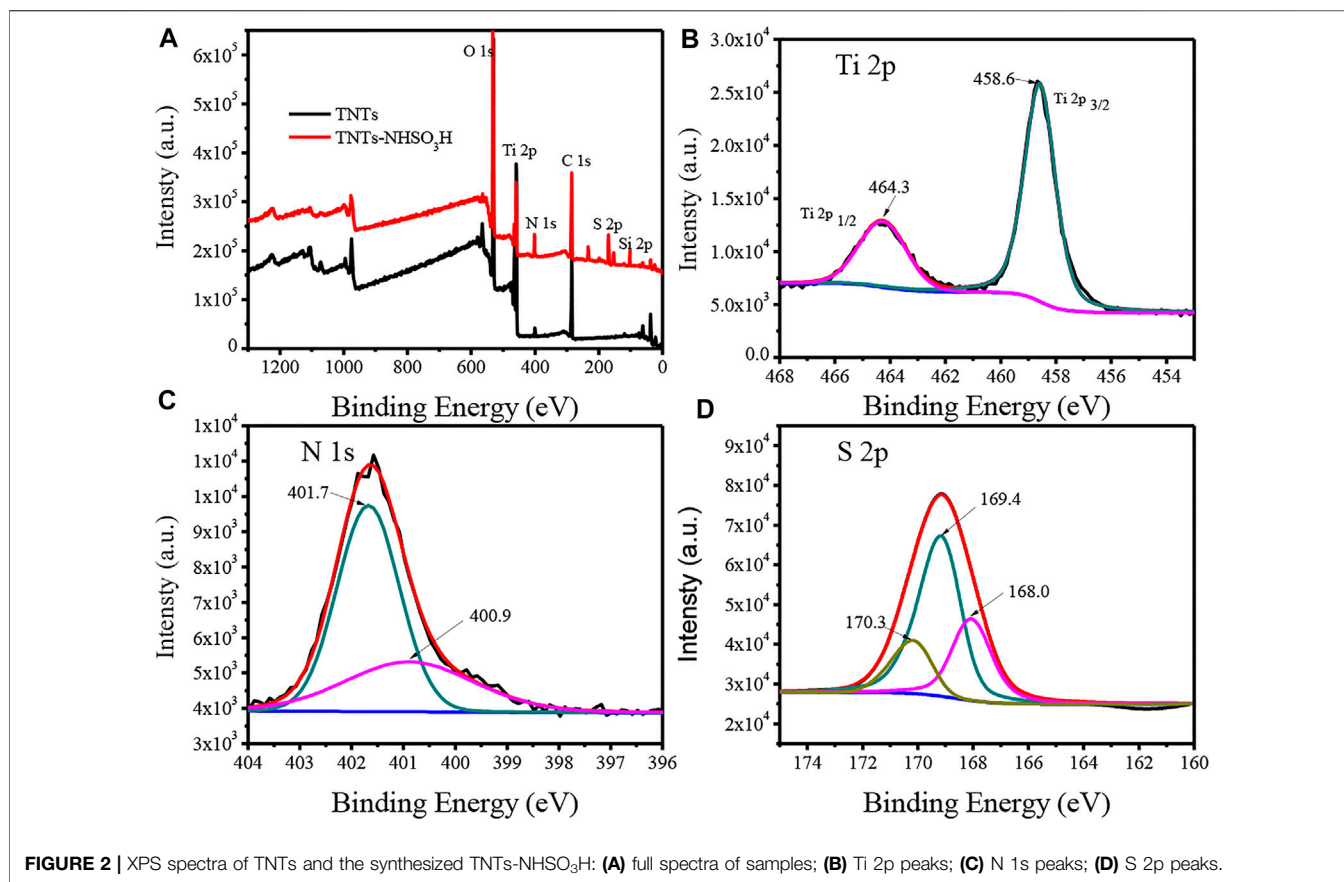
Materials

TiO_2 nanoparticles (anatase, >99.9%), 3-aminopropyltrimethoxysilane (APTMS), LA, and FA were purchased from Aladdin (Shanghai, China) and used as received. Toluene was purchased from Sinopharm Chemical Reagent Co., Ltd. (Shanghai, China) and was freshly distilled before use. Other reagents were of analytical grade and used without further purification. Experimental water was prepared by a Millipore Milli-Q pure water system.

Catalyst Preparation

Preparation of TNTs

TNTs were synthesized by a hydrothermal synthesis method, according to the reported literature with some slight



modifications (Kasuga et al., 1999). 2.0 g of TiO₂ nanoparticles with a particle size of 60 nm were mixed with 60 ml of 10 mol/L NaOH aqueous solution, followed by hydrothermal treatment at 150 C in a Teflon-lined autoclave for 24 h. After cooling, the treated powders were thoroughly washed with 0.1 mol/L HCl and water until the pH value of the washing solution reached 7.0, and subsequently filtered by 0.22 μm filters and dried one night at 80 C under vacuum. The obtained material is labeled as TNTs.

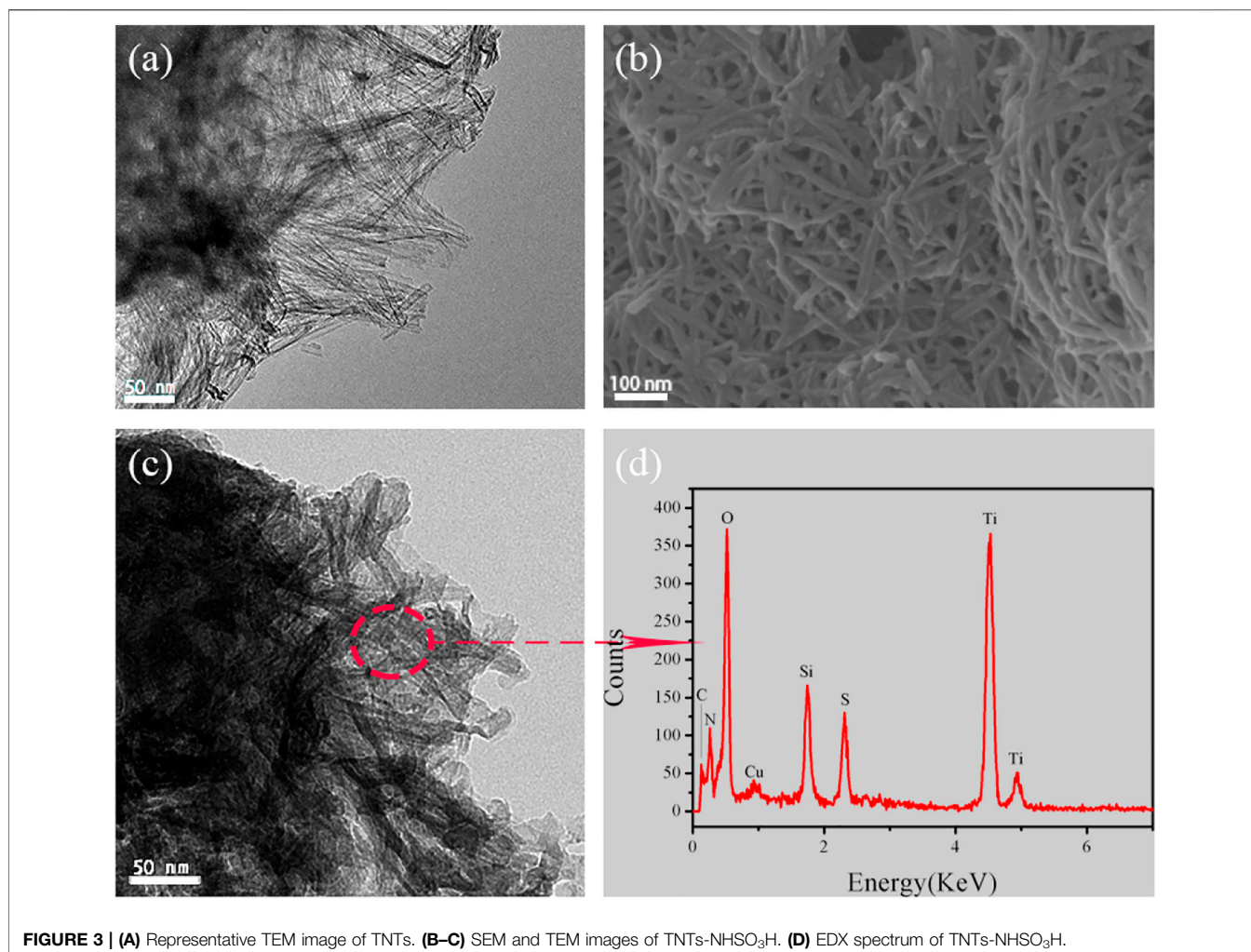
Preparation of TNTs-NHSO₃H

1 g of TNTs was suspended in 20 ml of dry toluene in a 50 ml round-flask and then 3-amino-propyltrimethoxysilane was added. The mixture was refluxed by stirring for 24 h. After the reaction was finished, the solid product was collected by centrifugation, washed three times with chloroform and acetone, respectively, and then dried in a vacuum oven at 80°C. The obtained solid powder was preloaded with 30 ml of dry dichloromethane in a suction flask equipped with a constant-pressure dropping funnel. A certain amount of chlorosulfonic acid was added dropwise over a period of 30 min at room temperature while the mixture was stirred slowly in an ice bath. After the addition was completed, the mixture was further stirred for 4 h. Then, the dichloromethane was removed, and the solid sample was washed with ethanol and

dried in a vacuum at 70 C. The resultant solid was designed as TNTs-NHSO₃H.

Characterization

Fourier transform infrared spectra (FT-IR) of the samples were collected by the KBr pellet technique on a Nicolet 370 infrared spectrophotometer (Thermo Nicolet, American) in the range 500–4,000 cm⁻¹. X-ray photoelectron spectroscopy (XPS) was tested by a Thermo fisher scientific using Mono Al Kα radiation, and binding energies were calibrated at 12.0 kV and 6.0 mA, respectively. The morphologies of the catalyst were investigated by using transmission scanning microscopy (TEM) with an acceleration voltage of 200 kV (JEOL 2100, Japan). The surface morphology of the TNTs-NHSO₃H catalyst was observed using a scanning electron microscope (SEM, Carl Zeiss Sigma-HD). X-ray diffraction (XRD) studies were carried out using a Bruker diffractometer with Cu Kα radiation to survey the crystal structure over a 2θ range of 10–80°. N₂ adsorption-desorption isotherms were recorded with an ASAP 2400 physisorption instrument made by Micromeritics Corporation (American). Prior to measurement, all samples were dried under vacuum at 333 K for 24 h. Pore size distribution was calculated using the Barrett-Joyner-Halenda (BJH) method. Thermogravimetric analysis (TGA) curves were



recorded in airflow on a Netzsch Model STA 409 PC instrument with a heating rate of 20K/min from room temperature to 973 K using α -Al₂O₃ as the standard material. The number of acid sites in each sample was determined by the acid-base titration method.

Catalytic Test

Esterification of LA With *n*-Butanol

In a typical procedure, the mixture of LA (3 mmol) and *n*-butanol (30 mmol) together with the catalyst (5 wt% of LA) were added to a round-bottom flask and was heated at the required reaction temperature in an oil bath under solvent-free condition. At periodic intervals, 0.2 ml of the reaction solution was withdrawn and centrifuged to separate the catalyst and was analyzed by Gas chromatography (GC).

Alcoholysis of FA With *n*-Butanol

In a typical run, 1 mmol of FA and 5 ml of *n*-butanol together with a prescribed amount of the catalyst were added to a 25 ml round bottom flask equipped with a reflux condenser under atmospheric pressure. The round bottom flask was heated in an oil bath at reaction temperatures ranging from 90–120°C. At periodic intervals,

the reaction mixture was withdrawn and centrifuged to separate the catalyst and was analyzed by Gas chromatography (GC).

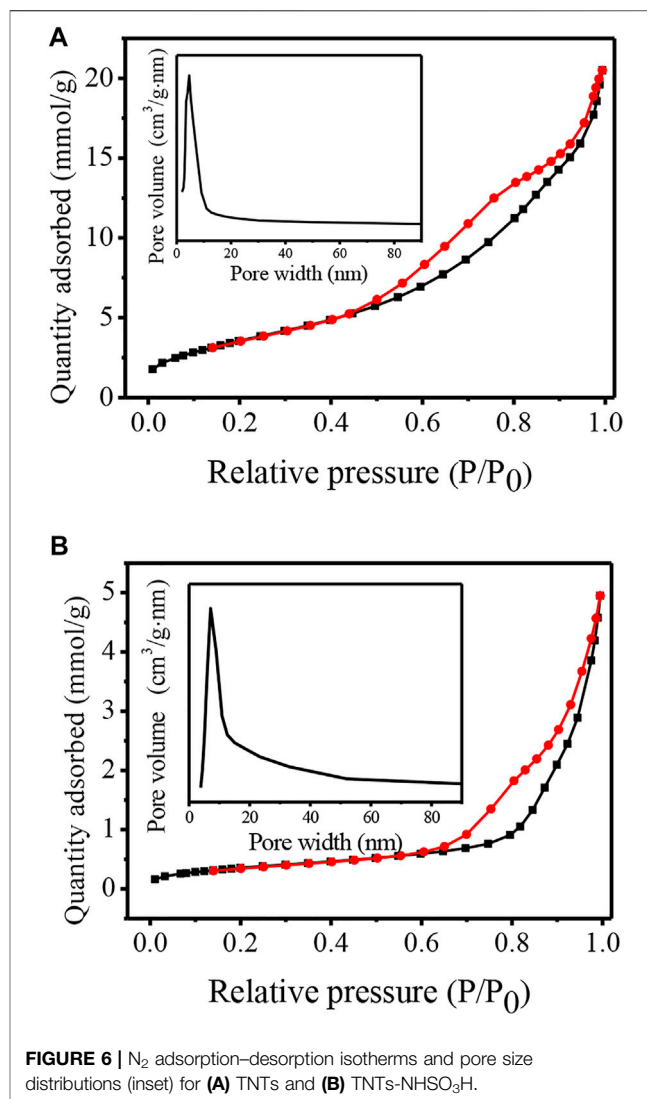
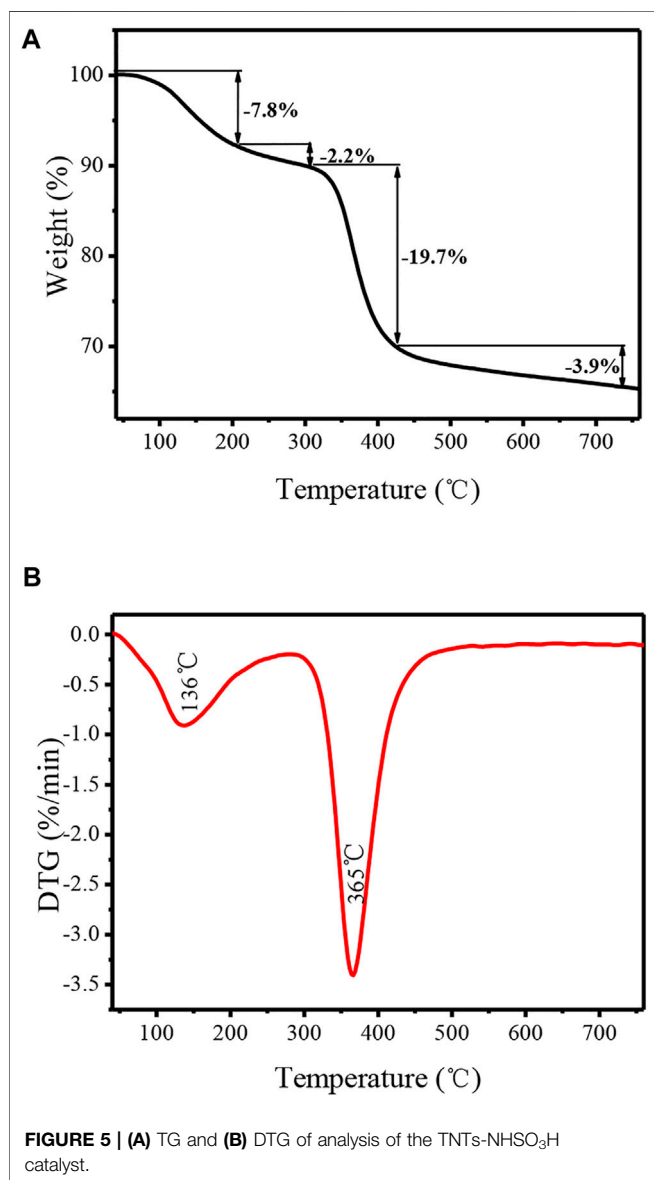
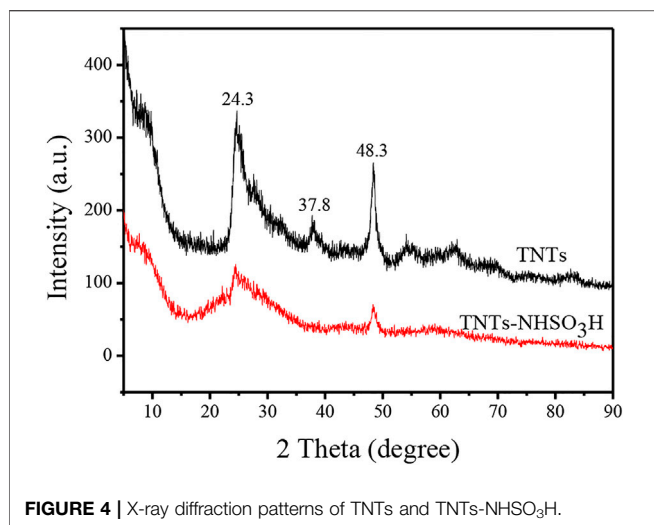
Reaction Intermediates Analysis

The reaction intermediates were identified by GC-MS, a Shimadzu GC system equipped with a capillary (30 m length, 0.32 mm internal diameter, 0.25 μ m film thickness). Mass spectrometer conditions were: ionization mode: EI, electron energy 70 eV; interface temperature: 250°C; ion source temperature: 200°C; mass scan range: 40–640 m/z, solvent delay 3.0 min. The flow rate of the carrier gas (helium) was 1.0 ml min⁻¹. A split ratio of 1:50 was used for the injection of 0.2 μ l of the solutions. The NIST05 S.LIB library was used for the mass spectrum analysis.

RESULTS AND DISCUSSION

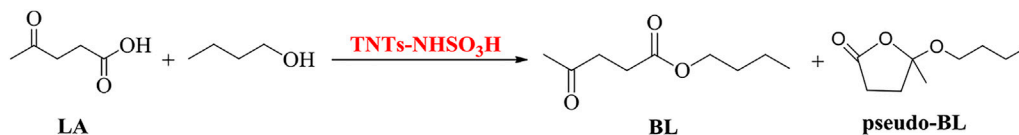
Characterization of Catalyst

FT-IR spectra for TNTs and TNTs-NHSO₃H samples are presented in **Figure 1**. Generally, the broad peak present

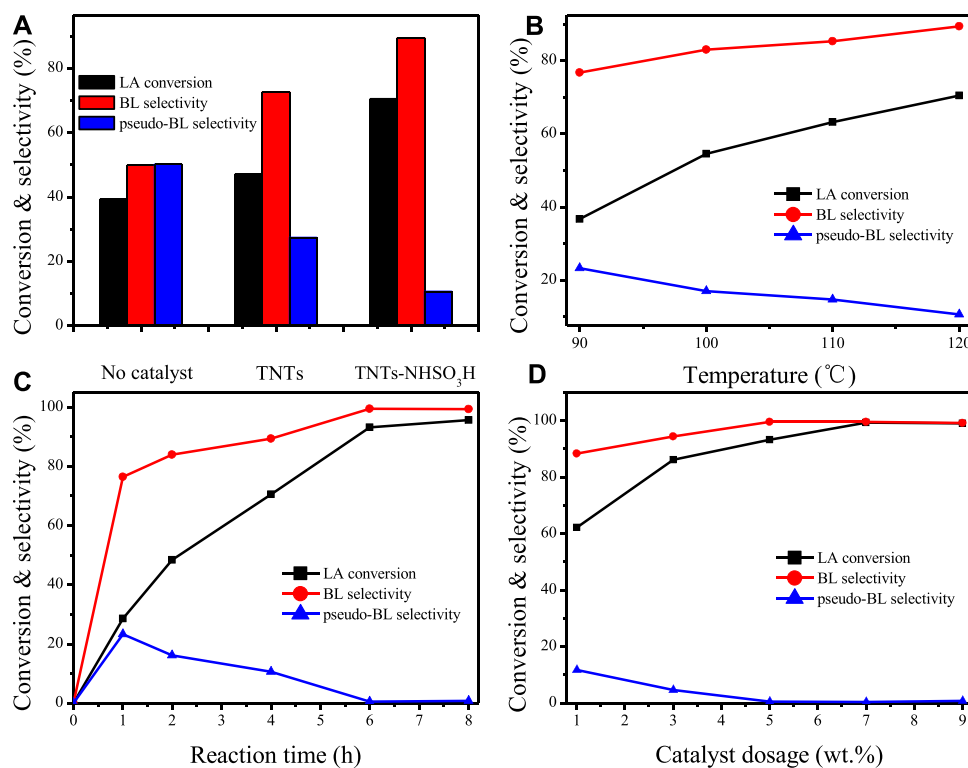


around 3,214–3,600 cm^{-1} and the low-intensity peak at 1,630 cm^{-1} are attributed to the stretching vibration of interlayer water molecules and surface OH groups, respectively. In the case of TNTs, the band below 1,200 cm^{-1} is attributed to Ti-O-Ti vibration and the peak around 490 cm^{-1} can be interpreted as the crystal lattice vibration of TiO₆ octahedra (Silva et al., 2017). The new absorption peaks in the frequency range of 2,800–2,960 cm^{-1} in the TNTs-NHSO₃H catalyst are ascribed to the C-H vibration of the aminopropyl segment (Pontón et al., 2014). The peak around 986 cm^{-1} could be interpreted as the Ti-O-Si band. Meanwhile, the band at 1,039 cm^{-1} is ascribed to Si-O stretching vibration. The peaks at 1,128 cm^{-1} and 1,224 cm^{-1} can be assigned to the sulfonyl moiety groups formed by the reaction of chlorosulfonic acid with amino groups (Kassae et al., 2011).

The surface chemical compositions and bonding environments for TNTs and TNTs-NHSO₃H were further analyzed by X-ray photoelectron spectroscopy (XPS), and the results are shown in Figure 2. From the full scan XPS



SCHEME 2 | Esterification of LA with *n*-butanol over the TNTs-NHSO₃H catalyst.

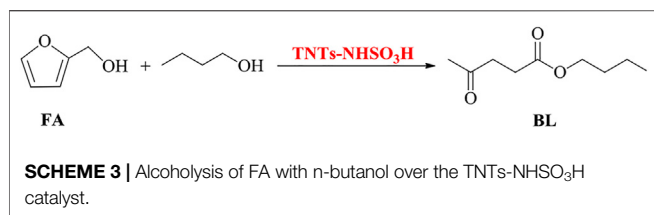


of samples, it can be seen that the TNTs-NHSO₃H sample is composed of C, N, O, S, Si, and Ti elements (**Figure 2A**), which are consistent with the elements expected to be obtained by the preparation route. **Figure 2B** shows the Ti 2p spectra of the TNTs-NHSO₃H sample. The binding energy of Ti 2p at 458.6 and 464.3 eV is correspond to the Ti 2p_{3/2} and Ti 2p_{1/2}, respectively. The binding energy of Ti 2p in the catalyst is consistent with that of pure TNTs, supporting that the oxidation state of Ti in the as-prepared TNTs-NHSO₃H is IV (Wang et al., 2018). As can be found in **Figure 2C**, the N 1s signal can be resolved into two peaks. The peak located at 400.9 eV can be assigned to the typical nitrogen present in APTMS. Another peak located at 401.7 eV for the N 1s peak can reasonably be attributed to N-S bonds (Kaid et al., 2020). **Figure 2D** depicts the XPS spectra of S 2p of TNTs-NHSO₃H. It is observed that S 2p has a strong peak at 169.4 eV, which is the characteristic peak of typical S=O bonds (Veisi et al., 2016).

Two peaks located at 168.0 and 170.3 eV can be assigned to the S-O and S-N, respectively (Song et al., 2015). These results indicate the formation of the desired catalytic system.

The acid amount of the catalyst was determined by the ion-exchanged method using an aqueous solution saturated with NaCl as an exchange agent. The acid density of TNTs-NHSO₃H is up to 2.27 mmol/g, which implies that a certain amount of Brønsted acidity sites can be constructed on the surface of TNTs.

The morphology of TNTs and TNTs-NHSO₃H was revealed by SEM and TEM, and the results are displayed in **Figure 3**. As illustrated by the TEM images, the TNTs sample shows the uniform open-ended tubes can be long up to several hundred nanometers (**Figure 3A**). It is worthy to note that the morphology of tubes in TNTs-NHSO₃H was still maintained (**Figures 3B,C**). The surface of titanate nanotubes was coated with a layer of silicon dioxide in the presence of dry toluene, which is the result



of the silanization of surface OH groups with APTMS. This means that more acidity sites can be constructed and immobilized on the TNTs surface by the following functionalization of amino groups in organ siloxane agents. According to the EDX spectrum of an area in **Figure 3C**, there are five elements, C, N, O, S, Si, and Ti, which can be ascertained in the TNTs-NHSO₃H (**Figure 3D**). The percent of N and S is 7.5 and 7 wt%, respectively. This result is consistent with the result previously obtained by XPS, indicating the material was successfully fabricated using a post-synthesis modification strategy.

The XRD pattern of the TNTs and TNTs-NHSO₃H are displayed in **Figure 4**. The TNTs had an XRD pattern that corresponds to the anatase crystal phase of titania. The peak exhibited at a 2θ value of 9.8 indicates the presence of a layered crystal structure formed in the hydrothermal process. It can be seen that all other diffraction peaks at the 2θ value of around 24.3°, 37.8°, and 48.3° are typical characteristic peaks of TNTs (Lu

et al., 2017). The XRD pattern of the as-prepared TNTs-NHSO₃H catalyst can well match the characteristic diffraction peaks of TNTs. It should be noted that there is a slight decrease in the intensity ratios of different peaks, which may be caused by the surface modification during the preparation process.

In order to further study the surface modification of TiO₂ nanotubes by organic functional groups, the catalyst was characterized by a thermogravimetric analyzer, and the obtained thermogravimetric curves are presented in **Figure 5**. It can be seen that a significant weight loss in the range of 100–200°C can be attributed to the elimination of water molecule which was physically adsorbed on the surface and into the pores of TNTs. An endothermic peak with a maximum of 136°C can be observed on the corresponding DTG curve. Also, there is a slight weight loss in the range of 200–300°C, which possibly corresponds to the dehydroxylation of TNTs. This phenomenon is consistent with the reported values for the TNT material (Preda et al., 2015). There is an obvious weight loss that started at 300°C, which is mainly attributed to the decomposition of the covalently bound organic functional groups from TNTs-NHSO₃H. The weight loss of approximately 19.7% in the range of 300–430°C is due to the removal of the organic motif. Furthermore, a strong and sharp endothermic DTG signal was observed at 365°C. In addition, the observed weight loss of approximately 3.9% occurs between 430 and 600°C which may be related to the thermal decomposition of

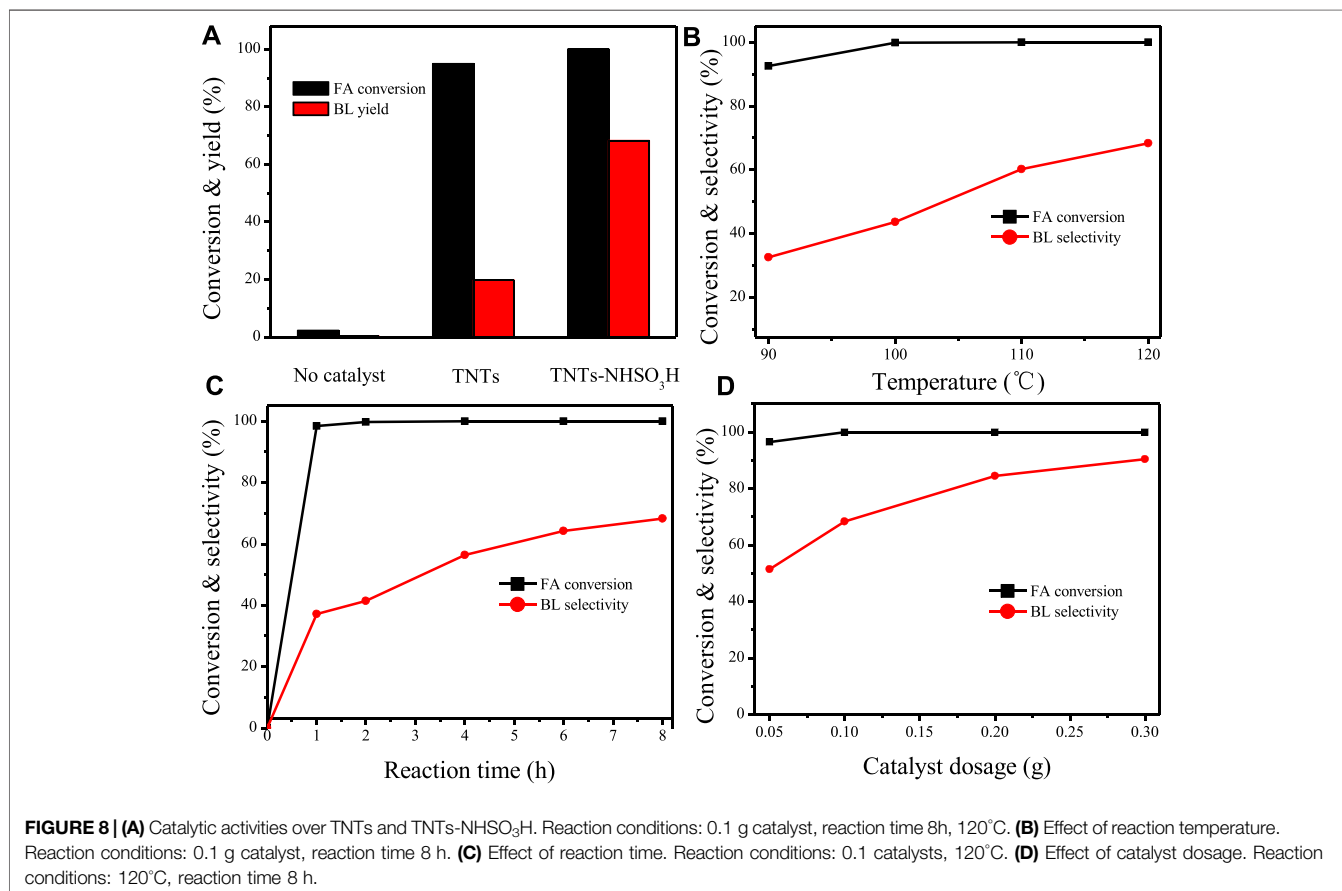
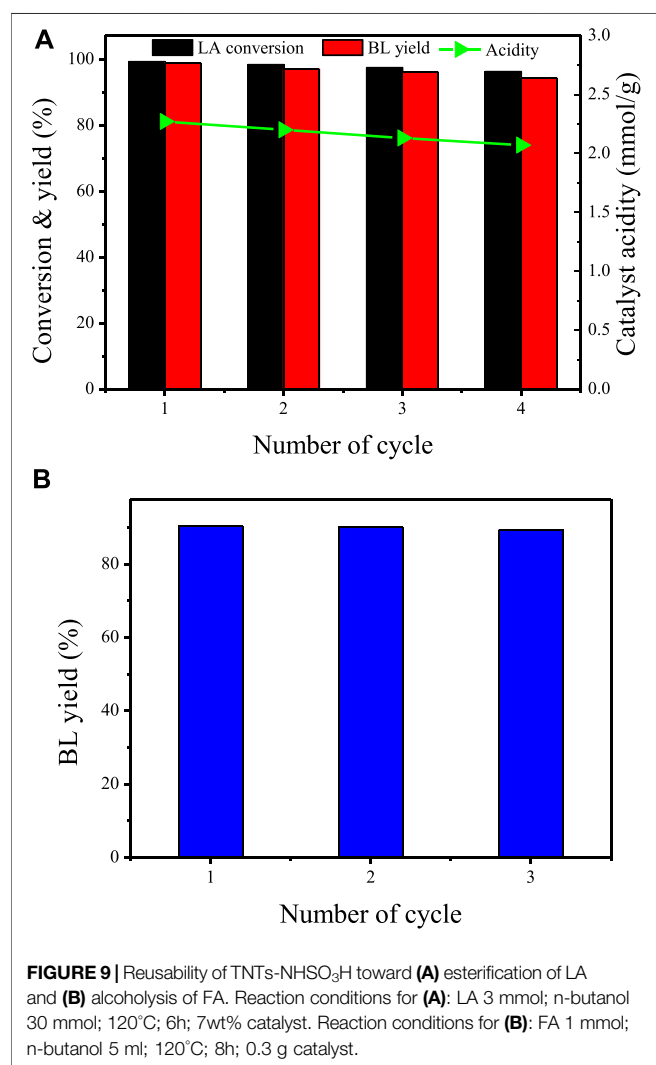


TABLE 1 | Comparison of TNTs-NHSO₃H with the reported catalyst.

Catalyst	Substrate	Temp. (°C)	Time (h)	BL yield (%)	Ref
TNTs-NHSO ₃ H	LA	120	6	98.9	This work
Meso-ZSM-5	LA	120	5	82.2	Morawala et al. (2019)
H ₃ PW ₁₂ O ₄₀ /Al-MCM-41	LA	120	4	90.0	Najafi Chermahini and Nazeri, (2017)
Sulfonated glucose-derived amorphous carbon	LA	100	4	90.5	Yang et al. (2018)
SnTUD ₁	LA	120	4	90.5	Pachamuthu et al. (2019)
NER@3DOM/m-OS	LA	40	12	74.6	Zhou S et al. (2018b)
TNTs-NHSO ₃ H	FA	120	8	90.4	This work
SMWP	FA	120	5	90.6	Yang et al. (2020)
[MIMBS] ₅ [AlW ₁₂ O ₄₀]	FA	120	6	94	Hao et al. (2017)
UiO-66(Hf)-SO ₃ H	FA	120	4	72	Gupta and Kantam, (2019)
KCC-1/Pr-SO ₃ H	FA	120	3	81.9	Mohammadbagheri and Najafi Chermahini, (2018)
GC-PTSA-AC	FA	120	4	91.0	Yang et al. (2019)



the organic residues. From the TG/DTG analysis, it is understood that the TNTs-NHSO₃H catalyst has greater thermal stability,

which confirms that it can be used for organic reaction temperatures below 300°C.

Figure 6 shows the N₂ adsorption-desorption isotherms and the corresponding pore size distribution curves of TNTs and TNTs-NHSO₃H. According to IUPAC classification, the TNT material exhibits the typical type IV isotherm with a hysteresis loop, confirming the mesoporous nature of TNTs. The surface area of TNTs is 300 m²/g. As shown in **Figure 6A**(inset), the pore size distribution presents the maximum positioned at 4.6 nm, corresponding to the inner nanotubular cavity of TNTs. This result suggests that TNTs had a uniform nanotubular structure. After functionalization of the parent material, the remarkable change in the N₂ adsorption-desorption isotherm curve was observed in **Figure 6B**. It is worth noting that the surface area of TNTs-NHSO₃H decreased to 29 m²/g. It is inferred that a part of the organosiloxane agents was confined inside the nanotubes, especially near the ends of the nanotubes, as TNTs possess a large fraction of voids in the interior, which resulted in the partial blocking of the tubular channel of TNTs-NHSO₃H. Although the BET surface area of TNTs-NHSO₃H is decreased in comparison to that of pure TNTs, it is still favorable for the acid-catalyzed reactions due to the more accessible acidic sites on the inside or outside of TNTs.

Catalytic Performances

Esterification of LA With *n*-Butanol

The catalytic performance of TNTs-NHSO₃H was first tested for the esterification of LA with *n*-butanol (**Scheme 2**) and the results are illustrated in **Figure 7**. The reaction products, *n*-butyl levulinate (BL) and *pseudo-n*-butyl levulinate (*pseudo*-BL) were detected by GC-MS techniques. Similar results were also observed by several authors (Ciptonugroho et al., 2016; Chaffey et al., 2021). As shown in **Figure 7A** remarkable catalytic performance of TNTs-NHSO₃H was observed since LA conversion (70.5%) with high selectivity (89.4%) to BL was achieved. The appearance of Brønsted acid centers in the TNTs-NHSO₃H catalyst is the primary reason for higher catalytic performance. To appraise the effects of reaction temperature, systematic studies were carried out at different temperature ranges from 90 to 120°C for 4 h (**Figure 7B**). The relative increase in both the LA conversion and BL selectivity was obtained when the

temperature was raised from 90 to 120°C. This result suggests that the relatively high reaction temperature is favorable for the conversion of *pseudo*-BL to BL and thereby improving the selectivity of BL. It should be noted that TNTs-NHSO₃H showed good catalytic activity at 120°C giving high conversion and high selectivity. **Figure 7C** shows the reaction time on LA conversion and BL selectivity in the range of 1–8 h at 120°C. It is found that the LA conversion and BL selectivity was increased with reaction time. A relatively high selectivity (99.5%) at 93.2% LA conversion was achieved after 6 h. However, there was no significant increase in conversion or yield with further prolonged time to 8 h. The effect of catalyst dosage on the conversion and yield was estimated while keeping the other variables constant and the results are plotted in **Figure 7D**. It was found that the LA conversion and the BL yield increased with the increasing amount of the catalyst. The optimum catalyst weight was found to be 7 wt% with 99.3% LA conversion because the further increase of the amount of catalyst exhibited a slight increment in conversion as well as yield.

Alcoholysis of FA With *n*-Butanol

The catalytic performance of the TNTs-NHSO₃H catalyst was further tested by synthesis of *n*-butyl levulinate from FA (**Scheme 3**) and the results are illustrated in **Figure 8**. A 19.7% yield of BL was achieved in the presence of the TNT sample. The catalytic activity of the TNTs was attributed to the number of Lewis acidic sites on its surface (Kitano et al., 2010). It is important to mention that the catalyst TNTs-NHSO₃H exhibited high activity for alcoholysis of FA with *n*-butanol giving a high yield of BL (**Figure 8A**). Based on this result, the effects of the variable parameters, including reaction temperature, reaction time, and catalyst dosage on the alcoholysis of FA to BL were investigated. As illustrated in **Figure 8B**, the BL yield was strongly affected by the reaction temperature. At a low reaction temperature (90°C), the BL yield was relatively low (32.5%). However, when the reaction temperature was increased from 90 to 120°C, the yield of BL increased significantly. This is because the higher reaction temperature facilitates the conversion of FA into BL. However, when the reaction temperature was further increased, there was no significant increase in the BL yield. This may be attributed to the undesired side reactions that occurred at higher temperatures (Huang et al., 2016). **Figure 8C** displayed the effect of reaction time on the production of BL. Complete conversion was reached around 1 h, whereas the initial yield of BL was low. It is noteworthy that the yield of BL gradually increases with an increase in reaction time from 1–8 h. There is no remarkable change after 6 h, and the maximum yield (68.3%) was obtained at 8 h. As shown in **Figure 8D**, BL yield was highly affected by catalyst dosage. It can be easily found that by increasing the catalyst amount up to 0.3 g, the yield of BL reached 90.4% with 100% FA conversion. This clearly indicates the fact that the increase of the loading of catalyst provides the more available acidic sites, thereby promoting the conversion of intermediate product to the target product.

Additionally, the catalytic performance of TNTs-NHSO₃H was better than that of other systems listed in **Table 1**. It is clear from the table that TNTs-NHSO₃H worked as an acid catalyst exhibiting excellent catalytic performance in the synthesis of *n*-butyl levulinate

from both LA and FA. More works to tune the catalytic properties of the catalyst and to characterize the surface acid properties are underway.

Reusability

To understand the recyclability of TNTs-NHSO₃H, the consecutive runs under the optimum conditions were performed in the esterification of levulinic acid with *n*-butanol. After each cycle, the spent catalyst was recovered by centrifugation, washed with ethanol, and dried for the next run. As presented in **Figure 9A**, the activity loss of TNTs-NHSO₃H is neglectable after four cycles, and a yield of the desired product BL was still maintained at 95.6%. It is worthy to note that the acidity of the catalyst declined from 1.28 to 1.06 mmol g⁻¹ after four consecutive recycles. The FT-IR analysis of the spent catalyst (**Supplementary Figure S1**) also confirmed that the active functional groups of the catalyst were relatively stable, providing the evidence for heterogeneous nature of TNTs-NHSO₃H. In addition, repeated runs of the alcoholysis reaction of FA with *n*-butanol were carried out under the above optimum conditions, and the results are displayed in **Figure 9B**. It was found that the catalyst was reused with a slight decrease in BL yield. This may be due to the black carbonaceous species, formed by the polymerization of the FA (Zhu et al., 2017), decreasing the accessibility of the substrates to the active sites.

CONCLUSION

In this study, titanate nanotubes were obtained through hydrothermal synthesis and then covalently linked sulfamic groups through the APTMS grafting and chlorosulfonic acid as a sulfonating reagent. The catalyst was fully characterized by various physicochemical characterization techniques, and the corresponding results suggest that the strong sulfonic acid groups were successfully grafted on the titanate nanotube surface. The as-prepared TNTs-NHSO₃H catalyst was used as a Brønsted solid acid for the synthesis of *n*-butyl levulinate from LA and FA. The excellent acid catalytic performance was observed in the synthesis of *n*-butyl levulinate from both the esterification of LA and the alcoholysis of FA under mild conditions. These results demonstrated that the obtained catalyst can be utilized as a potential candidate for the synthesis of LAEs and other value-added chemicals from biomass.

DATA AVAILABILITY STATEMENT

The original contributions presented in the study are included in the article/**Supplementary Material**, further inquiries can be directed to the corresponding author.

AUTHOR CONTRIBUTIONS

SZ: conceived and designed the research and produced the original manuscript, project administration. ML: investigation, writing-original draft preparation, data curation. JB: formal

analysis, writing-original draft preparation. XL: conceived and designed the research, writing-review editing, supervision. LW: methodology, formal analysis. ML: validation, data analysis. KH: catalyst characterization, DY: designed the research.

FUNDING

This work was supported by the Key Scientific Research Fund of Hunan Provincial Education Department (Grant No.19A035)

REFERENCES

- Adeleye, A. T., John, K. I., Adeleye, P. G., Akande, A. A., and Banjoko, O. O. (2021). One-Dimensional Titanate Nanotube Materials: Heterogeneous Solid Catalysts For Sustainable Synthesis Of Biofuel Precursors/Value-Added Chemicals—A Review. *J. Mater. Sci.* 56, 18391–18416. doi:10.1007/s10853-021-06473-1
- Alonso, D. M., Bond, J. Q., and Dumesic, J. A. (2010). Catalytic Conversion of Biomass to Biofuels. *Green. Chem.* 12, 1493–1513. doi:10.1039/c004654j
- Chaffey, D. R., Bere, T., Davies, T. E., Apperley, D. C., Taylor, S. H., and Graham, A. E. (2021). Conversion of Levulinic Acid to Levulinate Ester Biofuels by Heterogeneous Catalysts in the Presence of Acetals and Ketals. *Appl. Catal. B: Environ.* 293, 120219. doi:10.1016/j.apcatb.2021.120219
- Chao, H.-P., Lee, C.-K., Juang, L.-C., and Hsieh, T.-Y. (2013). Sorption of Organic Compounds with Different Water Solubility on Octadecyltrichlorosilane-Modified Titanate Nanotubes. *J. Taiwan Inst. Chem. Eng.* 44, 111–116. doi:10.1016/j.jtice.2012.08.005
- Christensen, E., Williams, A., Paul, S., Burton, S., and McCormick, R. L. (2011). Properties and Performance of Levulinate Esters as Diesel Blend Components. *Energy Fuels.* 25, 5422–5428. doi:10.1021/ef201229j
- Ciptonugroho, W., Al-Shaal, M. G., Mensah, J. B., and Palkovits, R. (2016). One Pot Synthesis of WO/mesoporous-ZrO₂ Catalysts for the Production of Levulinic Acid Esters. *J. Catal.* 340, 17–29. doi:10.1016/j.jcat.2016.05.001
- Démolis, A., Essayem, N., and Rataboul, F. (2014). Synthesis and Applications of Alkyl Levulinates. *ACS Sustainable Chem. Eng.* 2, 1338–1352. doi:10.1021/sc500082n
- de Carvalho, D. C., Oliveira, A. C., Ferreira, O. P., Filho, J. M., Tehuacanero-Cuapa, S., and Oliveira, A. C. (2017). Titanate Nanotubes as Acid Catalysts for Acetalization of Glycerol with Acetone: Influence of the Synthesis Time and the Role of Structure on the Catalytic Performance. *Chem. Eng. J.* 313, 1454–1467. doi:10.1016/j.cej.2016.11.047
- Duong, H. P., Hung, C.-H., Dao, H. C., Le, M. D., and Chen, C.-Y. (2018). Modification of TiO₂ Nanotubes with 3-aminopropyl Triethoxysilane and its Performances in Nanocomposite Coatings. *New J. Chem.* 42, 8745–8751. doi:10.1039/c8nj00642c
- Gaurav, N., Sivasankari, S., Kiran, G., Ninawe, A., and Selvin, J. (2017). Utilization of Bioresources for Sustainable Biofuels: A Review. *Renew. Sustainable Energy Rev.* 73, 205–214. doi:10.1016/j.rser.2017.01.070
- Gupta, S. S. R., and Kantam, M. L. (2019). Catalytic Conversion of Furfuryl Alcohol or Levulinic Acid into Alkyl Levulinates Using a Sulfonic Acid-Functionalized Hafnium-Based Mof. *Catal. Commun.* 124, 62–66. doi:10.1016/j.catcom.2019.03.003
- Hao, R., He, J., Zhao, L., and Zhang, Y. (2017). HPAs and POM-Based ILS Catalyzed Effective Conversion of Furfuryl Alcohol to Alkyl Levulinate. *ChemistrySelect.* 2, 7918–7924. doi:10.1002/slct.201701675
- Huang, Y.-B., Yang, T., Zhou, M.-C., Pan, H., and Fu, Y. (2016). Microwave-Assisted Alcoholysis of Furfural Alcohol into Alkyl Levulinates Catalyzed by Metal Salts. *Green. Chem.* 18, 1516–1523. doi:10.1039/c5sgc01581b
- Kaid, M. M., Gebreil, A., El-Hakam, S. A., Ahmed, A. I., and Ibrahim, A. A. (2020). Sulfamic Acid Incorporated HKUST-1: A Highly Active Catalyst and Efficient Adsorbent. *RSC Adv.* 10, 15586–15597. doi:10.1039/d0ra01063d
- Kassae, M. Z., Masrouri, H., and Movahedi, F. (2011). Sulfamic Acid-Functionalized Magnetic Fe₃O₄ Nanoparticles as an Efficient and Reusable

and Collaborative Innovation Center of New Chemical Technologies for Environmental Benignity and Efficient Resource Utilization.

SUPPLEMENTARY MATERIAL

The Supplementary Material for this article can be found online at: <https://www.frontiersin.org/articles/10.3389/fchem.2022.894965/full#supplementary-material>

- Catalyst for One-Pot Synthesis of α -amino Nitriles in Water. *Appl. Catal. A: Gen.* 395, 28–33. doi:10.1016/j.apcata.2011.01.018
- Kasuga, T., Hiramatsu, M., Hoson, A., Sekino, T., and Niihara, K. (1999). Titanate Nanotubes Prepared by Chemical Processing. *Adv. Mater.* 11, 1307–1311. doi:10.1002/(sici)1521-4095
- Kitano, M., Nakajima, K., Kondo, J. N., Hayashi, S., and Hara, M. (2010). Protonated Titanate Nanotubes as Solid Acid Catalyst. *J. Am. Chem. Soc.* 132, 6622–6623. doi:10.1021/ja100435w
- Li, S., Li, N., Li, G., Li, L., Wang, A., Cong, Y., et al. (2015). Protonated Titanate Nanotubes as a Highly Active Catalyst for the Synthesis of Renewable Diesel and Jet Fuel Range Alkanes. *Appl. Catal. B: Environ.* 170–171, 124–134. doi:10.1016/j.apcatb.2015.01.022
- Liu, X., Yang, W., Zhang, Q., Li, C., and Wu, H. (2020). Current Approaches to Alkyl Levulinates via Efficient Valorization of Biomass Derivatives. *Front. Chem.* 8, 794. doi:10.3389/fchem.2020.00794
- Lu, S.-x., Zhong, H., Mo, D.-m., Hu, Z., Zhou, H.-l., and Yao, Y. (2017). A H-Titanate Nanotube with superior Oxidative Desulfurization Selectivity. *Green. Chem.* 19, 1371–1377. doi:10.1039/c6gc03573f
- Mohammadbagheri, Z., and Najafi Chermahini, A. (2018). KCC-1/Pr-SO₃H as an Efficient Heterogeneous Catalyst for Production of N-Butyl Levulinate from Furfuryl Alcohol. *J. Ind. Eng. Chem.* 62, 401–408. doi:10.1016/j.jiec.2018.01.020
- Morawala, D., Dalai, A., and Maheria, K. (2019). Rice Husk Mediated Synthesis of Meso-Zsm-5 and its Application in the Synthesis of N-Butyl Levulinate. *J. Porous Mater.* 26, 677–686. doi:10.1007/s10934-018-0664-6
- Najafi Chermahini, A., and Nazeri, M. (2017). Esterification of the Levulinic Acid with N-Butyl and Isobutyl Alcohols over Aluminum-Containing MCM-41. *Fuel Processing Technology/Technol.* 167, 442–450. doi:10.1016/j.fuproc.2017.07.034
- Niu, H., and Cai, Y. (2009). Preparation of Octadecyl and Amino Mixed Group Modified Titanate Nanotubes and its Efficient Adsorption to Several Ionic or Ionizable Organic Analytes. *Anal. Chem.* 81, 9913–9920. doi:10.1021/ac901531k
- Pachamuthu, M. P., Srinivasan, V. V., Karvembu, R., and Luque, R. (2019). Preparation of Mesoporous Stannosilicates SnTUD-1 and Catalytic Activity in Levulinic Acid Esterification. *Microporous Mesoporous Mater.* 287, 159–166. doi:10.1016/j.micromeso.2019.05.061
- Pontón, P. I., d'Almeida, J. R. M., Marinkovic, B. A., Savić, S. M., Mancic, L., Rey, N. A., et al. (2014). The Effects of the Chemical Composition of Titanate Nanotubes and Solvent Type on 3-aminopropyltriethoxysilane Grafting Efficiency. *Appl. Surf. Sci.* 301, 315–322. doi:10.1016/j.apsusc.2014.02.071
- Preda, S., Rutar, M., Umek, P., and Zaharescu, M. (2015). A Study of thermal Properties of Sodium Titanate Nanotubes Synthesized by Microwave-Assisted Hydrothermal Method. *Mater. Res. Bull.* 71, 98–105. doi:10.1016/j.materresbull.2015.07.015
- Roy, P., Berger, S., and Schmuki, P. (2011). TiO₂ Nanotubes: Synthesis and Applications. *Angew. Chem. Int. Ed.* 50, 2904–2939. doi:10.1002/anie.201001374
- Shen, Q., Zhang, Y., Zhang, Y., Tan, S., and Chen, J. (2019). Transformations of Biomass-Based Levulinate Ester into γ -valerolactone and Pyrrolidones Using Carbon Nanotubes-Grafted N-Heterocyclic Carbene Ruthenium Complexes. *J. Energy Chem.* 39, 29–38. doi:10.1016/j.jechem.2019.01.007
- Silva, T. A., Diniz, J., Paixão, L., Vieira, B., Barrocas, B., Nunes, C. D., et al. (2017). Novel Titanate Nanotubes-Cyanocobalamin Materials: Synthesis and

- Enhanced Photocatalytic Properties for Pollutants Removal. *Solid State. Sci.* 63, 30–41. doi:10.1016/j.solidstatesciences.2016.11.008
- Song, D., An, S., Lu, B., Guo, Y., and Leng, J. (2015). Arylsulfonic Acid Functionalized Hollow Mesoporous Carbon Spheres for Efficient Conversion of Levulinic Acid or Furfuryl Alcohol to Ethyl Levulinate. *Appl. Catal. B: Environ.* 179, 445–457. doi:10.1016/j.apcatb.2015.05.047
- Tian, Y., Zhang, F., Wang, J., Cao, L., and Han, Q. (2021). A Review on Solid Acid Catalysis for Sustainable Production of Levulinic Acid and Levulinate Esters from Biomass Derivatives. *Bioresour. Technology.* 342, 125977. doi:10.1016/j.biortech.2021.125977
- Veisi, H., Taheri, S., and Hemmati, S. (2016). Preparation of Polydopamine Sulfamic Acid-Functionalized Magnetic Fe₃O₄ Nanoparticles with a Core/Shell Nanostructure as Heterogeneous and Recyclable Nanocatalysts for the Acetylation of Alcohols, Phenols, Amines and Thiols under Solvent-free Conditions. *Green. Chem.* 18, 6337–6348. doi:10.1039/c6gc01975g
- Wang, H., Zheng, L., Liu, G., and Zhou, Y. (2018). Enhanced Adsorption of Ag⁺ on Triethanolamine Modified Titanate Nanotubes. *Colloids Surf. A: Physicochemical Eng. Aspects.* 537, 28–35. doi:10.1016/j.colsurfa.2017.09.049
- Wang, L., Liu, W., Wang, T., and Ni, J. (2013). Highly Efficient Adsorption of Cr(VI) from Aqueous Solutions by Amino-Functionalized Titanate Nanotubes. *Chem. Eng. J.* 225, 153–163. doi:10.1016/j.cej.2013.03.081
- Wight, A. P., and Davis, M. E. (2002). Design and Preparation of Organic–Inorganic Hybrid Catalysts. *Chem. Rev.* 102, 3589–3614. doi:10.1021/cr101034m
- Wu, G., Shen, C., Liu, S., Huang, Y., Zhang, S., and Zhang, H. (2021). Research Progress on the Preparation and Application of Biomass Derived Methyl Levulinate. *Green. Chem.* 23, 9254–9282. doi:10.1039/d1gc03474j
- Yang, J., Ao, Z., Wu, H., Zhang, S., Chi, C., Hou, C., et al. (2020). Waste Paper-Derived Magnetic Carbon Composite: A Novel Eco-Friendly Solid Acid for the Synthesis of N-Butyl Levulinate from Furfuryl Alcohol. *Renew. Energ.* 146, 477–483. doi:10.1016/j.renene.2019.06.167
- Yang, J., Li, G., Zhang, L., and Zhang, S. (2018). Efficient Production of N-Butyl Levulinate Fuel Additive from Levulinic Acid Using Amorphous Carbon Enriched with Oxygenated Groups. *Catalysts.* 8, 14. doi:10.3390/catal8010014
- Yang, J., Zhang, H., Ao, Z., and Zhang, S. (2019). Hydrothermal Carbon Enriched with Sulfonic and Carboxyl Groups as an Efficient Solid Acid Catalyst for Butanolysis of Furfuryl Alcohol. *Catal. Commun.* 123, 109–113. doi:10.1016/j.catcom.2019.02.016
- Zhang, S., Li, J., Shang, N.-Z., Gao, S.-T., Wang, C., and Wang, Z. (2020). Conversion of Biomass-Derived Levulinate Esters to γ -Valerolactone with a Robust CuNi Bimetallic Catalyst. *New J. Chem.* 44, 15671–15676. doi:10.1039/d0nj02874f
- Zhou, L., He, Y., Ma, L., Jiang, Y., Huang, Z., Yin, L., et al. (2018). Conversion of Levulinic Acid into Alkyl Levulinates: Using Lipase Immobilized on Meso-Molding Three-Dimensional Macroporous Organosilica as Catalyst. *Bioresour. Technology* 247, 568–575. doi:10.1016/j.biortech.2017.08.134
- Zhou, S., Jiang, D., Liu, X., Chen, Y., and Yin, D. (2018). Titanate Nanotubes-Bonded Organosulfonic Acid as Solid Acid Catalyst for Synthesis of Butyl Levulinate. *RSC Adv.* 8, 3657–3662. doi:10.1039/c7ra12994g
- Zhou, S., Lai, J., Liu, X., Huang, G., You, G., Xu, Q., et al. (2022). Selective Conversion of Biomass-Derived Furfuryl Alcohol into N-Butyl Levulinate over Sulfonic Acid Functionalized TiO₂ Nanotubes. *Green. Energ. Environ.* 7, 257–265. doi:10.1016/j.gee.2020.09.009
- Zhou, S., Liu, X., Lai, J., Zheng, M., Liu, W., Xu, Q., et al. (2019). Covalently Linked Organo-Sulfonic Acid Modified Titanate Nanotube Hybrid Nanostructures for the Catalytic Esterification of Levulinic Acid with N-Butyl Alcohol. *Chem. Eng. J.* 361, 571–577. doi:10.1016/j.cej.2018.12.111
- Zhu, S., Guo, J., Wang, X., Wang, J., and Fan, W. (2017). Alcoholysis: A Promising Technology for Conversion of Lignocellulose and Platform Chemicals. *ChemSusChem.* 10, 2547–2559. doi:10.1002/cssc.201700597

Conflict of Interest: The authors declare that the research was conducted in the absence of any commercial or financial relationships that could be construed as a potential conflict of interest.

Publisher's Note: All claims expressed in this article are solely those of the authors and do not necessarily represent those of their affiliated organizations, or those of the publisher, the editors, and the reviewers. Any product that may be evaluated in this article, or claim that may be made by its manufacturer, is not guaranteed or endorsed by the publisher.

Copyright © 2022 Zhou, Lei, Bai, Liu, Wu, Long, Huang and Yin. This is an open-access article distributed under the terms of the Creative Commons Attribution License (CC BY). The use, distribution or reproduction in other forums is permitted, provided the original author(s) and the copyright owner(s) are credited and that the original publication in this journal is cited, in accordance with accepted academic practice. No use, distribution or reproduction is permitted which does not comply with these terms.